

# UC Berkeley

## UC Berkeley Previously Published Works

### Title

Long-Term Variability of Soil Moisture in the Southern Sierra: Measurement and Prediction

### Permalink

<https://escholarship.org/uc/item/693270t9>

### Journal

Vadose Zone Journal, 17(1)

### ISSN

1539-1663

### Authors

Oroza, Carlos A  
Bales, Roger C  
Stacy, Erin M  
[et al.](#)

### Publication Date

2018

### DOI

10.2136/vzj2017.10.0178

Peer reviewed

# Long-Term Variability of Soil Moisture in the Southern Sierra: Measurement and Prediction

Carlos A. Oroza,\* Roger C. Bales, Erin M. Stacy, Zeshi Zheng, and Steven D. Glaser

C.A. Oroza, R.C. Bales, Z. Zheng, and S.D. Glaser, Dep. of Civil and Environmental Engineering, Univ. of California, Berkeley, CA 94720; R.C. Bales and E.M. Stacy, Sierra Nevada Research Institute, Univ. of California, Merced, CA 95343. \*Corresponding author (coroza@berkeley.edu).

Using 6 yr (Water Year [WY] 2009–WY 2014) of hourly in situ measurements from a spatially distributed water-balance cluster, we quantified the long-term accuracy of an algorithm used to predict spatial patterns of depth-integrated soil-water storage within the rain–snow transition zone of the southern Sierra Nevada. The algorithm—the multivariate, non-parametric regression-tree estimator Random Forest—was used to predict soil-water storage based on a combination of attributes at each instrument cluster (soil texture, topographic wetness index, elevation, northness, and canopy cover). Out-of-bag  $R^2$  (similar to cross-validation for Random Forest) was used to quantify the accuracy of the estimator for unobserved data. Accuracy was consistently high during the wet-up, snow-cover, and early recession periods of average and wet years. The accuracy declined at the end of a 3-yr dry period, and the relative rank of the independent variables in the model shifted. Soil texture was the highest-ranked independent variable across all years, followed by elevation and northness. Topographic wetness increased in importance during dry periods. Northness exhibited high importance during the wet-up and early recession periods of most water years. During dry years, the importance of elevation declined. In dry years, notable differences in soil-water storage at each depth include lower-than-average storage in the deeper regolith at the beginning of the water year and lower storage in near-surface layers during the winter resulting from transient snow cover.

Abbreviations: CART, classification and regression tree; CZO, Critical Zone Observatory; VWC, volumetric water content; WY, water year.

Predicting spatial patterns of soil-water storage in montane regions is confounded by complex topography, heterogenous subsurface properties, snow–soil interactions (Williams et al., 2009), maximum snow depth during the prior winter season (Molotch et al., 2009), and spatial variability of snow depth resulting in meter-scale runoff (Bales et al., 2011). Interannual patterns of precipitation and snowpack are also highly variable (Harrington et al., 1995), resulting in both inter- and intra-annual variability of the processes governing the spatial distribution of soil moisture. Although

passive-microwave monitoring enables remote observation of surface soil moisture, it is too coarse to capture spatial variability in the complex terrain of montane regions (Bales et al., 2006). Remotesensing techniques also capture only near-surface soil-moisture storage (Njoku et al., 2003; Wagner et al., 2007). Observing only near-surface storage is insufficient for understanding controls on ecological functioning, as tree roots and thus root-water uptake occur well below the surface (Bales et al., 2011). Thus a major challenge is estimating deeper soil-water storage from spatially extensive remotely sensed measurements.

Recent advances in low-cost sensor networks are enabling the deployment of spatially extensive in situ soil-moisture measurements at deeper soil layers than are accessible from remote sensing. These deeper in situ measurements could be combined with remotely sensed terrain attributes to predict soil-water storage at un-instrumented regions in a basin. Developing a strategic and systematic approach for in situ observation networks requires understanding the long-term accuracy of these methods, as well as the inter- and intraannual controls on soil moisture. As the amount and timing of water entering the soil exhibit considerable interannual variability, predictors designed to extrapolate in situ soil-water storage in average water years may not work well for years that are significantly wetter or drier. While there have been limited reports of catchment-scale soil-moisture variability in these regions (Williams et al., 2009; Bales et al., 2011), a long-term study of the accuracy of spatial soil-water storage estimates has not been reported. It is presently unclear how long-term variability will affect the accuracy, and relative independent-variable ranking, of soil-moisture prediction.

In the present study, we used long-term records of soil-water storage at multiple depths to quantify the accuracy of an algorithm that predicts soil-water storage. In situ measurements of soil-water storage and soil texture were combined with remotely sensed topographic attributes using a statistical regression algorithm to predict soil-water storage at un-instrumented regions. The aims of the present study were to: (i) quantify inter- and intra-annual trends in the algorithm accuracy; (ii) identify which landscape attributes are most informative for predicting intra-annual and interannual patterns of soil moisture, and (iii) compare temporal soil-water storage patterns at each layer during wet and dry years to determine which sensor layer is most representative of overall soil-water storage.

## Methods

We used a 6-yr dataset of spatially distributed water-balance measurements at the Southern Sierra Critical Zone Observatory (CZO) in the Kings River basin. Soil moisture was measured at 10-, 30-, 60-, and 90-cm depths at 27

sensor-node locations and depth-integrated to compute spatial soil-water storage. The data included a very wet water year (2011), years with near- or above-average precipitation (2009–2010), and a record dry period (2012–2014). Annual precipitation values are summarized in Table 1.

The distribution of sensor nodes was designed to capture the variability of physiographic features expected to affect snow and soil-moisture variability (Bales et al., 2011). Soil-moisture variability has been found to be controlled by multiple factors, including soil texture, topographic wetness, spatial variability of snow depth, and solar radiation (Moore et al., 1993, 1988; Dunne and Black, 1970; Zaslavsky and Sinai, 1981; Western et al., 1999). Sensor nodes at the Southern Sierra CZO were placed into distinct high- and low-elevation clusters, and within each cluster, sensor nodes were designed to sample a variety of slopes, soil-texture values, and aspect (north, south, and flat). Additionally, node placements were designed to capture variability in canopy cover, with sensors placed in open, under-canopy, and drip-edge locations.

The statistical regression algorithm Random Forest was then used to predict soil-water storage at un-instrumented locations based on the in situ measurements and five independent variables at each node: column-average soil texture, topographic wetness, northness, elevation, and location with respect to the canopy. Random Forest was selected because it enables multivariate prediction from both continuous and categorical independent variables (e.g., soil texture and location with respect to canopy, respectively).

### Site Description and Data Collection

The Southern Sierra CZO is located in the Kings River basin of the Southern Sierra Nevada (Fig. 1). It is situated in a mixed-conifer forest east of Fresno, CA, and contains sensors distributed across the rain–snow transition. The region receives mainly rain below 1500-m and snow above 2200-m elevations (Bales et al., 2011). Soils are weakly developed and formed from decomposed granite (Dahlgren et al., 1997). Higher elevation soils have a hard soil–bedrock interface, whereas soils at lower elevations have a deeper paralithic contact (Bales et al., 2011).

Data were collected at distributed sensor clusters in the watershed (37.059° N, –119.192° W). Two sites are situated at the upper (1981 m) and lower (1745 m) elevations of the Providence Creek watershed, co-located with the upper and lower meteorological sites of the US Forest Service’s Kings River Experimental Watersheds project. Within each site are clusters of instruments distributed according to the predominant aspect. The Upper meteorological (met) site has three clusters, with north, south and flat

aspects. The Lower meteorological (met) site has two clusters (north and south facing). Each instrument cluster has five to seven nodes stratified by canopy (open, drip edge, and under canopy) and by tree species found at each aspect. The higher elevation site has a cluster of 17 nodes, and the lower elevation site has 10 nodes. Sensors were installed in December 2007.

Data control and storage are on a Campbell Scientific CR1000 datalogger with an AM16/32B multiplexer (Campbell Scientific). Snow depth was measured with an ultrasonic depth sensor with analog control from Judd Communications. Soil volumetric water content and soil temperature were measured using Decagon Device's (now METER Group) ECHO-TM (now equivalent to the 5TM). Daily soil-moisture storage,  $S(t)_i$  for each  $i$ th node was determined by depth-integrating the volumetric water content (VWC) within the 0- to 90-cm layers:

$$S(t)_i = \theta(t)_{10\text{cm}} \Delta z_{0-20\text{cm}} + \theta(t)_{30\text{cm}} \Delta z_{20-45\text{cm}} + \theta(t)_{60\text{cm}} \Delta z_{45-75\text{cm}} + \theta(t)_{90\text{cm}} \Delta z_{75-100\text{cm}} \quad [1]$$

where  $\Delta z$  represents the thickness of the soil layer to which the VWC value is applied.

The 90-cm sensors are installed only at a subset of nodes (16 total) owing to limitations on hand excavation for installations in rocky saprolite. Data for the present study are from the hourly Level-2 dataset, sampled four times each day (midnight, 06:00, 12:00, and 18:00) and were analyzed after formatting, calibration, and gap-filling by interpolation or regression.

Node locations were measured with a Trimble GeoXT GPS (horizontal accuracies between 0.6 and 1.4 m for points in the present study). Topographic properties at each node (elevation, slope, and aspect) were extracted from a lidar-derived digital elevation model of the region from the National Science Foundation's open topography database (opentopography.org, accessed September 2016). The grid size of the computed variables was 1 m (derived from an average of 11.65 returns per square meter).

Precipitation was collected using Belfort 5-780 rain gauges (Safeeq and Hunsaker, 2016). Evapotranspiration was measured at a nearby flux tower (Goulden et al., 2012; Rungee and Bales, 2017) (location shown in Fig. 1), and data were analyzed after gap filling.

### Soil-Moisture Prediction

To determine the long-term accuracy of soil-moisture prediction from the in situ measurements, we applied a regression-tree ensemble algorithm

(Random Forest; see Breiman, 2001) to the daily depth-integrated storage data. Classification and regression tree (CART) algorithms can be used to build predictors when independent variables are a mix of continuous and categorical features (e.g., topographic wetness index and location type in the present study). Ensemble tree algorithms such as Random Forest combine predictions from multiple CART models to arrive at an estimate of the true output. These methods have seen recent adoption in a variety of fields, such as land-cover classification (Gislason et al., 2006) and upscaling eddy-covariance measurements (Jung et al., 2009).

Five independent variables were used in the predictor for the present study: soil texture, topographic wetness, elevation, northness, and location type. Column-average soil-texture data for each node were extracted from a prior survey (see Table 2). Finer texture proportions (clay + silt) were used because they have been shown to affect soil-moisture variability at the hillslope scale (e.g., Famiglietti et al., 1998, Fig. 11b, who observed a generally high correlation coefficient between moisture content and clay content). Note that the texture of the lower elevation nodes is significantly finer than that at the higher elevation nodes. The topographic wetness index (TWI) was derived from the lidar elevation raster using the equation of Beven and Kirkby (1979):

$$TWI = \ln \frac{a}{\tan(b)} \quad [2]$$

where  $a$  is the upslope contributing area per unit contour and  $\tan(b)$  is the local slope. Topographic wetness was processed using the built-in module available at [opentopography.org](http://opentopography.org), which uses TauDEM (<http://hydrology.usu.edu/taudem>). Elevation was represented as an integer-based categorical variable representing the high- and low-elevation clusters because the elevation differences within the clusters are small compared with the elevation difference between the upper and lower clusters. Representing elevation as a categorical variable ensures that the feature importance measured by the algorithm represents differences between the high- and low-elevation clusters rather than meter-scale elevational differences within each cluster. Northness was computed from the lidar slope and aspect rasters (Molotch et al., 2004):

$$\text{northness} = \sin(\text{slope}) \times \cos(\text{aspect}) \quad [3]$$

Finally, location type was encoded as one of three categorical variables representing drip-edge, under-canopy, and open measurements. The node properties are summarized in Table 2.

We implemented the regression using the Random Forest module in Scikit-learn Version 19.0, an open-source Python-based package for machine learning (Pedregosa et al., 2011). Details and source code for the algorithms used in this study are available at [scikit-learn.org](http://scikit-learn.org).

A new regression was performed at the four daily intervals for each day in the 6-yr study period using all 27 nodes. The predictive accuracy of the algorithm was quantified using the out-of-bag  $R^2$  of the model. The out-of-bag  $R^2$  is computed from the unused samples in the randomly sampled set of independent and dependent variables. This is similar to a cross-validation procedure, which better quantifies the ability of the model to predict unseen data (Breiman, 2001). The relative importance of each independent variable was determined from the feature importance method of the predictor, which determines the relative contribution of each independent variable based on the error reduction resulting from a split on a given variable in CART predictor, averaged across all trees in the ensemble (Pedregosa et al., 2011).

The parameters of the Random Forest algorithm that have the largest influence on the accuracy and feature importance are the tree depth and the number of trees in the ensemble. Tree depth affects how many splits are performed within each tree in the ensemble. Deeper trees have a greater tendency to overfit data, increasing the accuracy on the training data but reducing the out-of-bag accuracy. A larger number of trees in the ensemble will mitigate the overfitting of any individual tree and will tend to produce more stable out-of-bag error estimates and feature importance measures (because these quantities will be derived from a greater number of splits on the independent variables). Fifty trees were used in the ensemble, and the threshold for the minimum number of samples required to be at a leaf node was set to 3. With these values, stable out-of-bag accuracy and independent variable ranking was observed. Increasing the minimum samples required to be at a leaf node was found to reduce the algorithm accuracy. The mean squared error criterion was used to determine split quality. The maximum number of independent variables was left as the default, which allows the algorithm to consider all independent variables when performing a split. The maximum tree depth was not set because the tree depth is controlled by the minimum samples on a leaf-node parameter. Bootstrapped samples were used when building trees (enabling out-of-bag error computation), and the out-of-bag score parameter was set to true. Other parameters were left as the defaults because they either implicitly control tree depth (which we already control by specifying the minimum samples at a leaf node), assume the use of weighted samples (all samples had even weight in the present study), or reuse a previous solution when building the ensemble (we built a new ensemble for each regression).

## Soil-Moisture Deviations by Layer

To determine which soil layer was most representative of total storage in a soil column during the study period, we computed an idealized storage value by using the VWC of the  $l$ th layer as a function of time,  $t$ , to represent the VWC of the entire profile,  $S(t)$ . We then compared this idealized storage for each layer with the actual measured storage. The layer with the deviation percentage,  $D_l$ , closest to 0 was determined to be the most representative layer. The deviation percentage for a given soil layer was computed as

$$D_l = 100 \left[ \frac{\theta_l(t)_\mu \Delta z_{0-100\text{cm}}}{S(t)_\mu} - 1 \right] \quad [4]$$

where  $\theta_l(t)_\mu$  is the mean of the VWC measurements across a set of nodes for the  $l$ th layer, and  $S(t)_\mu$  represents the mean total storage across the same node set (Eq. [1]). The deviation percentage will be zero if the depth-integrated value at the sensor layer matches the storage,  $S(t)_\mu$ , positive if the storage estimated from that layer exceeds  $S(t)_\mu$ , and negative if it is less than  $S(t)_\mu$ . In this computation, we considered only the subset of nodes with 90-cm-depth sensors and continuous records for all soil layers.

## Results

The average soil-moisture storage across all nodes in an average-precipitation year (WY 2009) is shown in Fig. 2. We discuss the results with respect to the wet-up, snow-cover, recession, and dry phases, which are labeled on the figure. The wet-up period occurs early in the water year (1 October 1–30 September), as initial precipitation inputs increase storage throughout the soil column. The snow-cover period occurs just after the first layers of snow begin to melt, typically in the months of November and December. Recession occurs just after the last of the snow cover has melted (typically mid-May). The inflection point during the dry-down process defines the beginning of the dry period.

The variability of soil-water storage is illustrated by the relative duration of each period in Fig. 3. Water Year 2009 had the closest to average precipitation of any year in the present study (Table 1). The longest period for these years is the snow-cover period (approximately 4 mo: mid-December–April), when soilwater storage averages about 25 to 30 cm; the shortest period is the dry period (approximately 2 mo: August and September), when soil-water storage averages about 10 cm (Fig. 3). Water Year 2011 was unusually wet: the snow-cover period was longer than in any other year (>5 mo), and there was no discernible dry period. The wet-up and snow-cover periods were notably shorter for drier-than-average years (2012–

2014), and dry periods were notably longer (up to 4 mo in the case of WY 2013).

### Soil-Moisture Prediction

The algorithm accuracy (out-of-bag  $R^2$ ) is high when soils are wet and declines when soils are dry (Fig. 3). The accuracy is consistently high during the snow-cover and early recession periods of average and wet years (2009–2011). Dry periods exhibit extended periods of low accuracy: the out-of-bag  $R^2$  declined to 0.3 or lower during the dry phase of each year. The lowest accuracy periods occurred during the wet-up phases of dry years (WY 2013–2014) when there was minimal snowpack and less precipitation than in average or wet years. Large changes to the snowpack state can result in a temporary decrease in accuracy, e.g., out-of-bag  $R^2$  decreased from 0.7 to 0.1 during an early-season melt event in 2009 and from 0.7 to 0.3 during melt events in 2010.

Soil texture is the highest ranking predictor of soil-water storage during snow-cover periods, with elevation and northness contributing as well. The importance of texture declines during early recession, with that of elevation and northness increasing. The importance of northness is typically highest during the wet-up phases of typical years, when soil pores are not near field capacity. In the late-recession and dry periods, northness exhibits some importance, but less than soil texture.

Topographic wetness becomes important as dry-down progresses and during dry years; however, the out-of-bag  $R^2$  is low during these periods. The importance of elevation is typically highest just as the last of the snowpack is melting, slightly earlier than topographic wetness. In dry years, the importance of elevation declined relative to prior years, although it regained importance during snow-on/snow-off periods in 2014. Finally, location type exhibits minimal importance in any year. The increase in its importance in 2013 should be disregarded, as it corresponds to a near-zero-accuracy period for the predictor.

### Differences in Soil-Water Storage at Each Layer during Dry vs. Wet Years

In comparing the temporal soil-moisture patterns in the driest year (WY 2014) with an average year (WY 2009), differences in the wet-up period were associated with drier lower soil layers, which are not affected by initial inputs of precipitation (Fig. 4). The figure shows the mean VWC for the subset of nodes containing 90-cm-depth sensors. Conditions at the end of the recession period were nearly identical in wet and dry years, reflecting depletion of root-accessible water at this depth. Lower layer soils were all just below 10% VWC. In wet years, early-season precipitation affected all soil

layers, resulting in a highly correlated response across the soil column. In WY 2014, shallow soil layers responded to precipitation, but lower soil layers remained dry well into the snow-cover period.

During the snow-cover period, interannual differences in the temporal patterns of soil moisture for each layer appear to have resulted from a transition to discontinuous snow cover during dry years (Fig. 5). Unlike the wet-up period, which was characterized by dry lower layer soils, upper soil layers during snow cover showed greater declines due to multiple winter-spring melt events. During the snow-off periods (second panel, Fig. 5), soil temperature and evapotranspiration increased (first and third panels of Fig. 5, respectively). This suggests that the more-rapid decline of water storage in the surface layers (10-cm layer compared with 60-cm layer in the third panel of Fig. 5) may be attributable to increased evaporation from upper soil layers during snow-off periods.

Decreased precipitation and transient snow cover in dry years affect how closely each soil layer tracks overall storage (Fig. 6). In most water years, the idealized storage using the 10-cm VWC underestimated true storage by approximately 25 to 30% by the end of the recession period. For dry years, underestimates are 40% or more for a longer portion of the water year. During the wet-up and early snow-cover periods of the driest year (2014), drier lower layer soils resulted in the 10-cm layer overestimating storage by >40%, which was not observed in average or wet years. As the dry years progressed, the idealized storage predicted from the 60-cm layer overestimated storage in dry periods to a greater degree than in average or wet years. Overall, the idealized storage using the 60-cm VWC is closest to depth-integrated storage across the clusters.

## Discussion

The variability of the predictor accuracy and independent variable ranking in the present study is in accord with the results of Western et al. (1999) and Williams et al. (2009), who found significant seasonal variability in the degree to which terrain indices explain the distribution of soil moisture. We found that topographic features exhibit predictable seasonal controls on soil moisture storage in average-precipitation years but are altered by drought conditions.

The high accuracy observed during wet periods in the present study is probably due to the fact that the soil was close to field capacity (therefore the spatial distribution of soil texture strongly controlled soil-water storage). Nonetheless, there are high-accuracy periods in which the importance of texture is low and other terrain attributes contribute significantly (e.g., the high importance of northness during wet-up periods and the high importance

of elevation during recession). We also found that the short-term predictive accuracy can decrease even when the soil is near field capacity (e.g., due to significant changes in the snowpack during January 2009 and 2010).

Other low-accuracy periods, such as during wet-up in 2013 and 2014, may have resulted from minimal precipitation input to exceptionally dry soils. The spatial distribution of soil water storage in these periods may be driven by spatial heterogeneity in precipitation and interception patterns rather than topographic features and texture. Given these findings, confidence in the statistical spatial prediction of daily soil-water storage from in situ sensors must incorporate knowledge of current and prior snowpack, precipitation, and soil-moisture conditions. Because the accuracy of the estimate is affected by the temporal variability of snow depth, deploying more-complete water-balance measurements (i.e., including snow-depth and air-temperature sensors) may be useful for quantifying the accuracy of the algorithm in real time.

Our results suggest that sensor-placement strategies must account for the relative importance of predictive features, which vary across seasons and years. Capturing the spatial variability of soil texture should be prioritized across all years. Sampling strategies focused on the wet-up period would benefit from a representative sampling of northness, and sampling strategies focused on the recession period should sample along an elevation transect. The relative importance of elevation declined in dry years, perhaps due to the decreasing differences in snowpack between the upper and lower elevation sites; therefore, sampling elevation gradients may be less important for dry years, except during transient snow-cover conditions. Location with respect to the canopy ("location type") did not appear to be important for the model in any period of any year. This is consistent with the findings of Bales et al. (2011), who observed little variability in soil moisture resulting from location with respect to tree canopy (Bales et al., 2011, Fig. 8b).

The increased importance of topographic wetness during dry periods is counter-intuitive, given that this variable is expected to be more informative for wet periods (Western et al., 1999). Because the increased importance of this variable occurs only in comparatively low-accuracy periods, this finding should be interpreted with caution.

The interannual variability of soil-water storage in the present study may also have implications for remote sensing, which measures only near-surface soil moisture. During normal and wet years, tightly coupled soil layers make observations of the surface storage a good proxy for lower level storage. In dry years, we observed greater decoupling of shallower and deeper soil

moisture storage, particularly during the wet-up and snow-cover periods. During the wet-up periods of dry years, minimal input precipitation resulted in near-surface soil moisture increasing more rapidly than in lower soil layers. In the snow-cover period of dry years, transient snowcover resulted in surface layers drying more rapidly than lower soil layers. Remote sensing tools may therefore overestimate soil-water storage in the lower soil column during the wet-up period of dry years and may underestimate soil-water storage in the lower soil column during transient snow-off conditions.

## Conclusion

There are three conclusions relevant to the aims of this study. First, a regression tree ensemble algorithm using topographic features and soil texture as independent variables exhibits higher accuracy in predicting depth-integrated water storage during wet years than during dry years. Second, soil texture has consistently high feature importance in the algorithm for predicting spatial soil-water storage across all years. Other landscape attributes exhibited seasonal trends: the importance of northness peaked during the wet-up period, and the importance of elevation and topographic wetness index peaked during the recession and dry periods. Third, the 60-cm layer tracked depth-integrated soil-water storage more closely than did the individual 10-, 30-, or 90-cm layers. Deviations of each layer from depth-integrated storage were exacerbated by transient snow-cover conditions during dry years, as well as lower-than-average deep soil storage in the wet-up period of the driest year, resulting in a decoupling of upper and lower layers of the soil column.

This study underscores the importance of in situ measurements for monitoring soil moisture in montane regions, which feature topographic complexity, heterogenous soil and vegetation properties, and coupled snow-soil interactions. Future studies could evaluate these methods using more in situ sensors deployed across greater elevation gradients in the rain-snow transition. It would be informative to deploy sensors that capture gradients in variables not included in this study, particularly to investigate features that could better predict soil moisture in dry years such as large biomass gradients. Future studies could also develop methods to synthesize the findings from this study into sensor placement and modeling strategies for basin-scale soil monitoring. Remote sensing, in situ, and deterministic modeling could then be combined to better predict soil-moisture storage in atypical water years. Finally, it would be beneficial to extend the representative-layer analysis to different regions to assess the applicability of these findings to other catchments.

## Acknowledgments

This research was supported by the National Science Foundation through the Southern Sierra Critical Zone Observatory (EAR-1331939), a Major Research Instrumentation grant (EAR-1126887), and the University of California Center for Information Technology Research in the Interest of Society. Soil-moisture data used in the present study are available from <https://dash.ucmerced.edu/stash/dataset/doi:10.6071/Z7WC73>. We wish to thank the members of the Southern Sierra Critical Zone Observatory for their constructive feedback, especially Toby O'Geen.

## References

- Bales, R.C., J.W. Hopmans, A.T. O'Geen, M. Meadows, P.C. Hartsough, P. Kirchner, et al. 2011. Soil moisture response to snowmelt and rainfall in a Sierra Nevada mixed-conifer forest. *Vadose Zone J.* 10:786–799. doi:10.2136/vzj2011.0001
- Bales, R.C., N.P. Molotch, T.H. Painter, M.D. Dettinger, R. Rice, and J. Dozier. 2006. Mountain hydrology of the western United States. *Water Resour. Res.* 42:W08432. doi:10.1029/2005WR004387.
- Beven, K.J., and M.J. Kirkby. 1979. A physically based, variable contributing area model of basin hydrology. *Hydrol. Sci. J.* 24:43–69. doi:10.1080/02626667909491834
- Breiman, L. 2001. Random forests. *Mach. Learn.* 45:5–32. doi:10.1023/A:1010933404324
- Dahlgren, R.A., J.L. Boettinger, G.L. Huntington, and R.G. Amundson. 1997. Soil development along an elevational transect in the western Sierra Nevada, California. *Geoderma* 78:207–236. doi:10.1016/S0016-7061(97)00034-7
- Dunne, T., and R.D. Black. 1970. An experimental investigation of runoff production in permeable soils. *Water Resour. Res.* 6:478–490. doi:10.1029/WR006i002p00478
- Famiglietti, J.S., J.W. Rudnicki, and M. Rodell. 1998. Variability in surface moisture content along a hillslope transect: Rattlesnake Hill, Texas. *J. Hydrol.* 210:259–281. doi:10.1016/S0022-1694(98)00187-5
- Gislason, P.O., J.A. Benediktsson, and R.J. Sveinsson. 2006. Random Forests for land cover classification. *Pattern Recognit. Lett.* 27:294–300. doi:10.1016/j.patrec.2005.08.011
- Goulden, M. L., R.G. Anderson, R. C. Bales, A.E. Kelly, M. Meadows, and G.C. Winston. 2012. Evapotranspiration along an elevation gradient in California's Sierra Nevada. *J. Geophys. Res.* 117:G03028. doi:10.1029/2012JG002027

- Harrington, R.F., K. Elder, and R.C. Bales. 1995. Distributed snowmelt modeling using a clustering algorithm. In: Biogeochemistry of seasonally snow-covered catchments. IAHS Publ. 228. IAHS Press, Wallingford, UK. p. 167-174.
- Jung, M., M. Reichstein, and A. Bondeau. 2009. Towards global empirical upscaling of FLUXNET eddy covariance observations: Validation of a model tree ensemble approach using a biosphere model. *Biogeosciences* 6:2001-2013. doi:10.5194/bg-6-2001-2009
- Molotch, N.P., P.D. Brooks, S.P. Burns, M. Litvak, R.K. Monson, J.R. McConnell, and K. Musselman. 2009. Ecohydrological controls on snowmelt partitioning in mixed-conifer sub-alpine forests. *Ecohydrology* 2:129-142. doi:10.1002/eco.48
- Molotch, N.P., T.H. Painter, R.C. Bales, and J. Dozier. 2004. Incorporating remotely-sensed snow albedo into a spatially-distributed snowmelt model. *Geophys. Res. Lett.* 31:L03501. doi:10.1029/2003GL019063
- Moore, I.D., G.J. Burch, and D.H. Mackenzie. 1988. Topographic effects on the distribution of surface soil water and the location of ephemeral gullies. *Trans. ASAE* 31:1098-1107. doi:10.13031/2013.30829
- Moore, I.D., T.W. Norton, and J.E. Williams. 1993. Modelling environmental heterogeneity in forested landscapes. *J. Hydrol.* 150:717-747. doi:10.1016/0022-1694(93)90133-T
- Njoku, E.G., T.J. Jackson, V. Lakshmi, T.K. Chan, and S.V. Nghiem. 2003. Soil moisture retrieval from AMSR-E. *IEEE Trans. Geosci. Remote Sens.* 41:215-229. doi:10.1109/TGRS.2002.808243
- Pedregosa, F., G. Varoquaux, A. Gramfort, V. Michel, B. Thirion, O. Grisel, et al. 2011. Scikit-learn: Machine learning in Python. *J. Mach. Learn. Res.* 12:2825-2830.
- Rungee, J. P., and R.C. Bales. 2017. Evapotranspiration response to multiyear dry periods in the semi-arid western United States. In: Abstracts, AGU Fall Meeting, New Orleans. 11-15 Dec. 2017. Am. Geophys. Union, Washington, DC.
- Safeeq, M., and C.T. Hunsaker. 2016. Characterizing runoff and water yield for headwater catchments in the southern Sierra Nevada. *J. Am. Water Resour. Assoc.* 52:1327-1346. doi:10.1111/1752-1688.12457
- Wagner, W., V. Naeimi, K. Scipal, R. de Jeu, and J. Martínez-Fernández. 2007. Soil moisture from operational meteorological satellites. *Hydrogeol. J.* 15:121-131. doi:10.1007/s10040-006-0104-6

Western, A.W., R.B. Grayson, G. Blöschl, G.R. Willgoose, and T.A. McMahon. 1999. Observed spatial organization of soil moisture and its relation to terrain indices. *Water Resour. Res.* 35:797–810. doi:10.1029/1998WR900065

Williams, C.J., J.P. McNamara, and D.G. Chandler. 2009. Controls on the temporal and spatial variability of soil moisture in a mountainous landscape: The signature of snow and complex terrain. *Hydrol. Earth Syst. Sci.* 13:1325–1336. doi:10.5194/hess-13-1325-2009

Zaslavsky, D. and G. Sinai. 1981. Surface hydrology: I. Explanation of phenomena. *J. Hydraul. Div., Am. Soc. Civ. Eng.* 107:1–16.

Table 1. Total annual precipitation in each water year for the present study. Data from a Belfort 5-780 rain gauge (Safeeq and Hunsaker, 2016). Mean annual precipitation for the study period is 129 cm.

Water year	Total precipitation
	cm
WY 2009	127
WY 2010	163
WY 2011	228
WY 2012	102
WY 2013	88
WY 2014	65

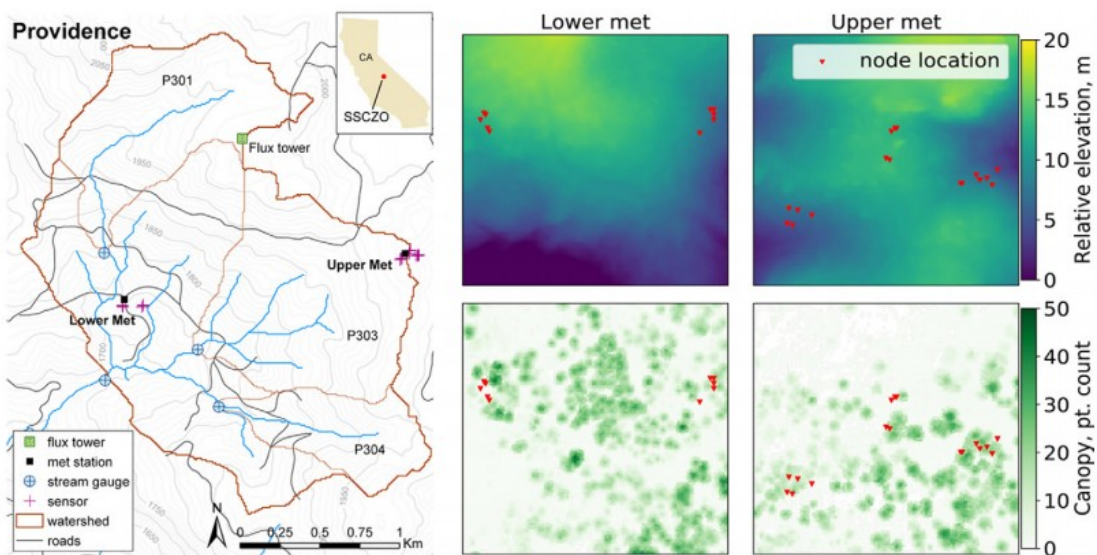


Fig. 1. Study site location and sensor distribution. Left-hand panel shows the Providence catchments, and the locations of the Upper meteorological (met) and Lower met clusters of sensor nodes within the basin. Right-hand panels show the distribution of sensors at Upper and Lower met locations with respect to the 1-m<sup>2</sup> lidar digital elevation model (top panels) and the canopy (bottom panels). Each panel is a 150- by 150-m area. Zero elevation corresponds to 1725 and 1970 m at the Lower and Upper met sites, respectively.

Table 2. Properties for each node (lidar-derived topographic variables and mean in situ texture measurements).

Node†	Texture‡	TWI§	Elevation (categorical)	Northness
Upper met				
N acde	27.13	6.48	high (1)	0.21
N acuc	23.88	7.14	high (1)	0.24
N cdde	19.42	4.52	high (1)	0.20
N cduc	14.06	7.91	high (1)	0.20
N open	22.72	5.19	high (1)	0.15
N plde	23.00	5.70	high (1)	0.13
N pluc	21.60	6.62	high (1)	0.23
S acde	19.94	5.96	high (1)	-0.29
S acuc	20.03	2.98	high (1)	-0.21
S open	16.40	3.62	high (1)	-0.14
S qkde	20.08	4.46	high (1)	-0.19
S qkuc	18.80	5.23	high (1)	-0.31
F acde	14.68	4.38	high (1)	0.01
F acuc	12.67	3.64	high (1)	0.02
F open	24.45	5.18	high (1)	0.06
F ppde	25.54	4.31	high (1)	-0.05
F ppuc	27.24	3.02	high (1)	-0.03
Lower met				
N acde	26.31	3.28	low (0)	-0.04
N acuc	30.78	9.39	low (0)	-0.07
N open	20.86	2.03	low (0)	-0.11
N cduc	33.31	1.87	low (0)	-0.01
N cdde	33.14	5.93	low (0)	-0.03
S cdde	37.35	2.76	low (0)	-0.15
S cduc	35.72	1.93	low (0)	-0.11
S open	36.20	5.66	low (0)	-0.16
S ppde	33.83	4.94	low (0)	-0.18
S ppuc	35.62	3.39	low (0)	-0.27

† Upper met soils are weakly developed, Lower met are well developed, containing more clay and silt; F, flat aspect; S, south-facing aspect; N, north-facing aspect; uc, under canopy; de, at the drip edge; ac, white fir [*Abies concolor* (Gord. & Glend.) Lindl. ex Hildebr.]; pp, ponderosa pine (*Pinus ponderosa* Lawson & C. Lawson); qk, California black oak (*Quercus kelloggii* Newberry); pl, sugar pine (*Pinus lambertiana* Douglas); cd, incense cedar [*Calocedrus decurrens* (Torr.) Florin].

‡ Texture data summarized from Bales et al. (2011).

§ Topographic wetness index.

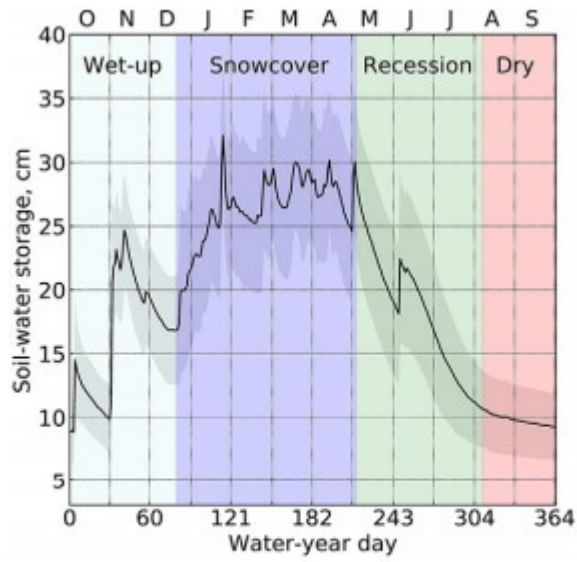


Fig. 2. Mean and standard deviation across all nodes of depth-integrated soil-water storage for an average-precipitation year (Water Year 2009).

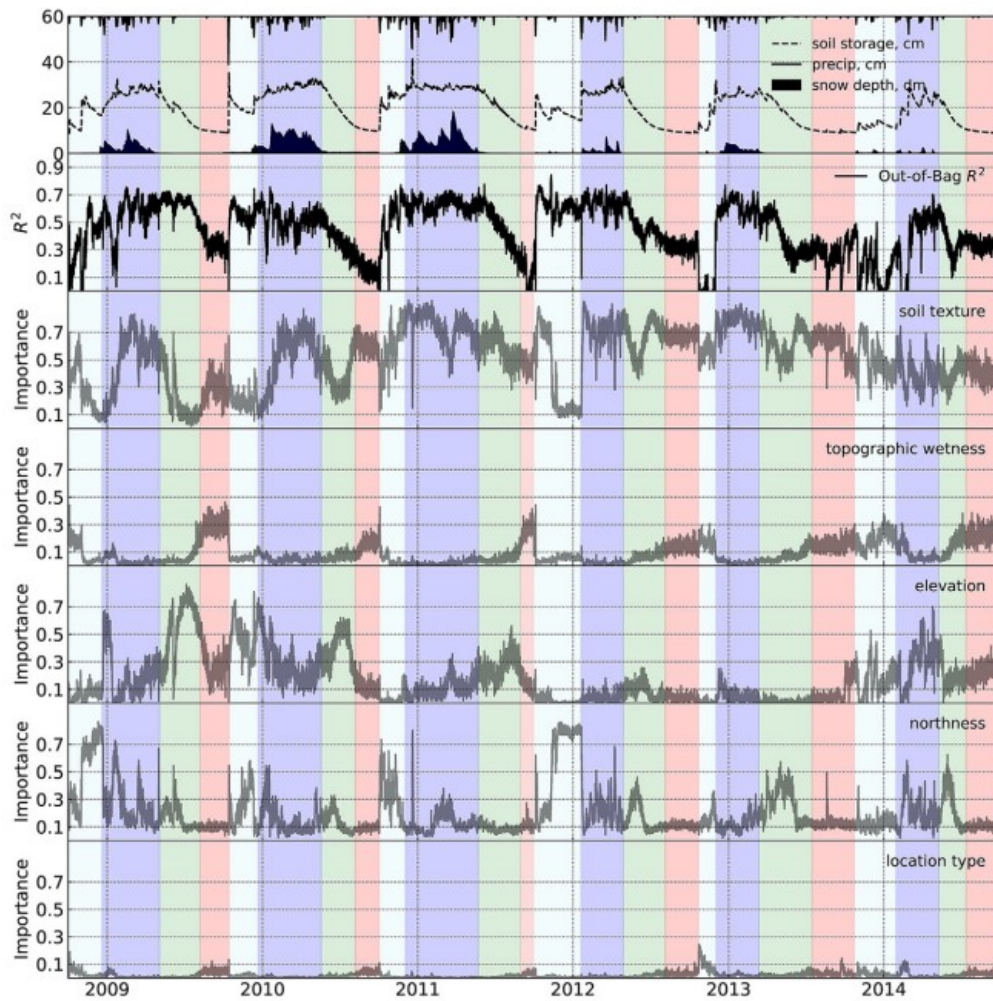


Fig. 3. Regression tree ensemble predictive accuracy and independent variable ranking for six water years. Top panel shows daily precipitation, mean soil-moisture storage, and mean snow depth from all nodes. Second panel shows predictive accuracy (out-of-bag  $R^2$ ) of the algorithm. The out-of-bag  $R^2$  better represents accuracy on unobserved data. Lower panels show the relative importance of each predictive variable, values for which sum to 1.0. As in Fig. 2, light blue is wet-up, dark blue is snow cover, green is recession, and red is dry.

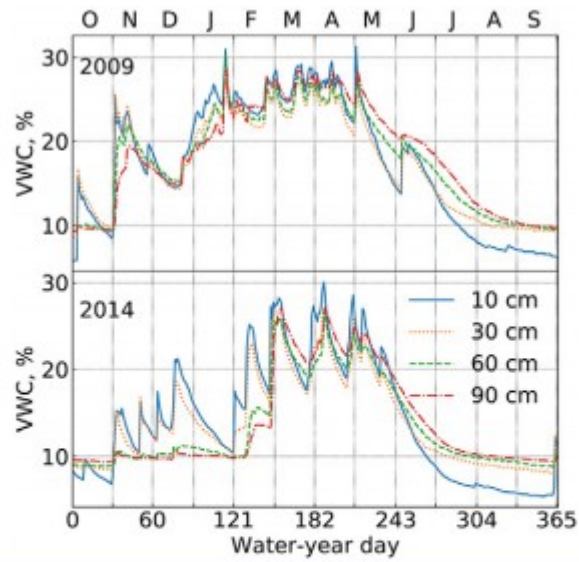


Fig. 4. Mean volumetric water content (VWC) at each layer from the node subset containing 90-cm-depth sensors in wet (2009) and dry (2014) years. In dry years, initial precipitation had minimal effects on lower levels of soil moisture, resulting in a decoupling of storage in the upper and lower layers.

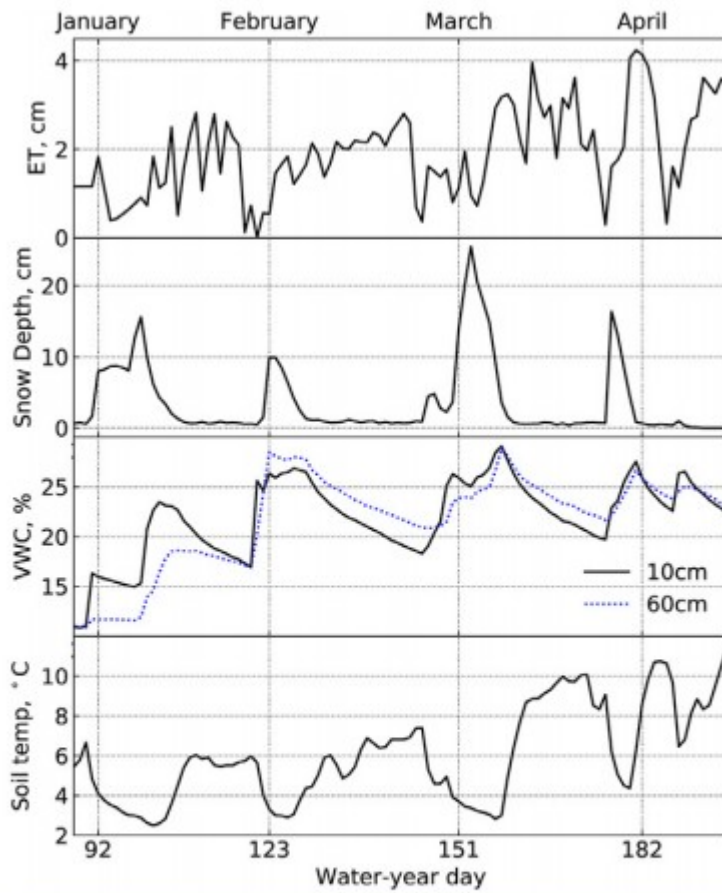


Fig. 5. Snow-off conditions during the 2014 snow-cover period resulting in soil-moisture storage decline, increased soil temperature, and evapotranspiration (ET). The lower three panels show mean snow depth, soil volumetric water content (VWC), and soil temperature patterns; the top panel shows evapotranspiration.

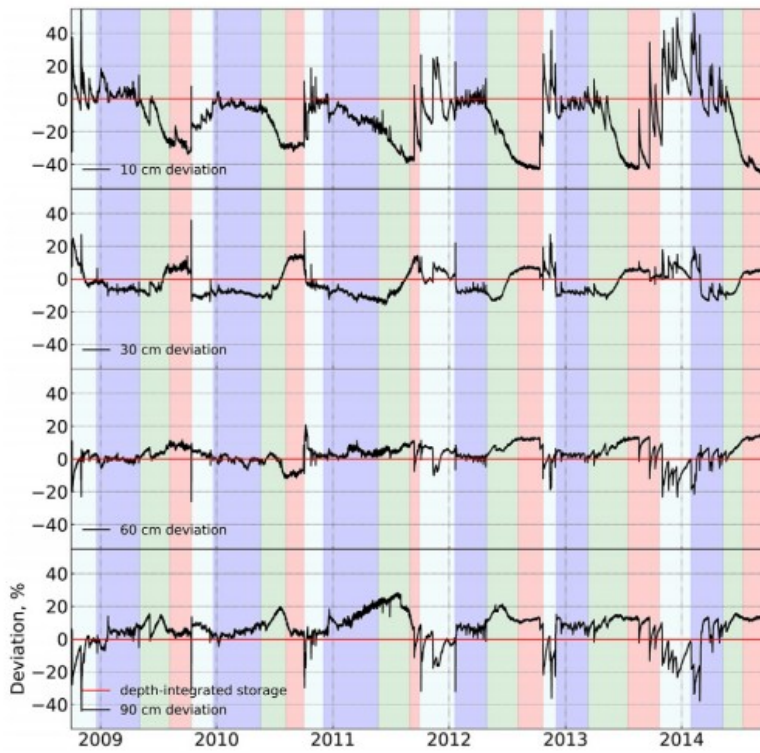


Fig. 6. Deviation of depth-integrated storage using each soil layer individually compared with the true depth-integrated storage. In dry years, 10-cm layers underestimated soil storage in the recession and dry period by a greater amount than in wet years. Storage was over-predicted by 10-cm layers during the wet-up periods of dry years due to drier-than-average lower layers. Across all years, the 60-cm layer was typically closest to soil-water storage.